



BIO_SOS

Project Title: **BIO_SOS Biodiversity Multisource Monitoring System:
from Space TO Species**

Contract No: FP7-SPA-2010-1-263435

Instrument:

Thematic Priority:

Start of project: 1 December 2010

Duration: 36 months

Deliverable No: D6.5

Report on habitat state and ecosystem status assessment

Due date of deliverable: 28 February 2013

Actual submission date: 10/04/2013

Version: 1st version

Main Authors: Mauro Rossi (P1-IRPI), Dino Torri (P1-IRPI), Fasma Diele (P1-IAC), Carmela Marangi (P1-IAC), Stefania Ragni (P1-IAC), Palma Blonda (P1-ISSIA), Harini Nagendra (P5) with contributions of Ivan Marchesini (P1-IRPI), Elisa Santi (P1-IRPI)



Project ref. number	263435
Project title	BIO_SOS: Biodiversity Multisource Monitoring System: from Space to Species

Deliverable title	Report on habitat state and ecosystem status assessment
Deliverable number	D6.5
Deliverable version	v1
Previous version(s)	V0
Contractual date of delivery	28 th February 2013
Actual date of delivery	10/04/2013
Deliverable filename	BIO_SOS_D6.5 _V1.doc
Nature of deliverable	R
Dissemination level	PU = Public
Number of pages	35
Workpackage	WP 6 Task 6.3
Partner responsible	Partner 1 (CNR)
Author(s)	Mauro Rossi (P1-IRPI), Dino Torri (P1-IRPI), Fasma Diele (P1-IAC), Carmela Marangi (P1-IAC), Stefania Ragni (P1-IAC), Harini Nagendra (P5) with contributions of Ivan Marchesini (P1-IRPI) ,Elisa Santi (P1-IRPI),
Editors	Carmela Marangi (P1-IAC) and Dino Torri (CNR-IRPI)
EC Project Officer	Florence Beroud

Abstract	The assessment of the ecosystem state, in terms of the functionality of the soil and of the soil/vegetation interactions is a relevant step of the procedures for monitoring the impact of human activities and climate changes on landscapes. The focus is here on the connectivity of the landscape with respect to the flux of different elements like water, sediment and fauna. The deliverable is organized into two parts: a) the first one introduces a new landscape, plants, landslides and erosion
-----------------	---

	<p>model, which exploits the Landscape Function Analysis framework to deal with the hydrogeological connectivity. As a result of the proposed methodology we provide an example of scenario analysis, applied to a BIO_SOS study site; b) the second one deals with the connectivity related to fauna fluxes. We introduce a new mathematical model, built on the metapopulation dynamics approach, to study predator-prey populations dynamics. The study has been motivated by the conservation issues related to the wolf-wild boar pair populating the Alta Murgia BIO_SOS study site.</p>
Keywords	<p>Ecosystem assessment, hydrogeological connectivity, soil/vegetation interactions, metapopulation models</p>

Signatures

Written by	Responsibility- Company	Date	Signature
Carmela Marangi and Dino Torri	Responsible of Task 6.3 (P1:CNR-IAC and CNR-IRPI)	29/03/2013	
Verified by			
Harini Nagendra	Leader of WP6 (P5)	8/04/2013	
Approved by			
Palma Blonda	Coordinator (P1)	10/04/2013	
Benedetto Biagi	Project Management Team - Quality Group (P1)	10/04/2013	

Table of Contents

1.	Executive summary	6
2.	Introduction.....	7
3.	Part I. Landscape, plants, landslides and erosion model (LANDPLANER).....	8
3.1	Effects of roads: a new tool developed in GRASS (r.sim.road)	8
3.2	NRCS Curve number method.....	9
3.3	A theoretical approach to describe gully head development by runoff	11
3.4	LANDPLANER description	12
3.5	Examples of scenario analyses	14
3.6	Part I. Conclusions	19
4.	Part II. Metapopulation dynamics: the effect of corridor size in spatially explicit/implicit models	20
4.1	Background.....	20
4.2	The spatially explicit model.....	22
4.3	The reduced spatially implicit model.....	24
4.4	The effect of corridor size variation: comparison between explicit and reduced implicit RM model	26
4.5	The effect of corridor size variation: comparison among different reduced implicit models ...	28
4.6	Part II. Conclusions and recommendations	33
5.	Appendix.....	34
5.1	Appendix 1: Acronym list	34
6.	References	35

1. Executive summary

Deliverable D6.5 is the output of WP6-Task 6.3 (start month 8, end-month 27) activity on ecosystem state assessment, and is related to the activity of WP5-Task 5.4 (start month 16, end month 30), on change detection and the activity of Task 6.5 (start month 8, end-month 30) on pressure scenario analysis.

The assessment of the ecosystem state, in terms of the functionality of the soil and of the soil/vegetation interactions is a relevant step of the procedures for monitoring the impact of human activities and climate changes on landscapes. The aim is not only to assess changes in the condition of landscape health over time but also to track recovery actions subsequent to landscape degradation, and to build landscape scenarios useful for management purposes.

The idea is to consider the landscape as a complex system with an internal organization finalized to capturing, distributing and sharing internal and external resources useful for running life. Part of the landscape functioning is to act as a reservoir of such resources, being capable to redistribute them through connecting regions. The connectivity of the system, i.e the capability to sustain the flux of the resources necessary to the biota, is what impacts the functionality of the landscape and its status. In turn, changes in the flux of different elements like water, sediment and fauna may deeply affect the connectivity of the habitat by increasing its fragmentation. Deriving a quantitative estimate of such changes and their impact on the landscape connectivity is among the objectives of the BIO_SOS project.

The deliverable is divided into two parts: the first one describes the methodology developed to analyze the responses of a landscape to rainfall by combining remote sensing data, in-field measurements and ancillary data in a new distributed model which takes into account the impact of roads on runoff, infiltrated water and erosion. An example of scenario analysis is performed on one BIO_SOS test site. The preliminary study is intended to provide evidence of the effectiveness of the approach to be used in Task 6.5, which can be extended to the other project test sites.

The second part deals with a peculiar aspect of the landscape connectivity related to the flux of fauna. We are concerned here with cyclic predator-prey populations as in the case of the wolf - wild boar pair which populates the Italian Alta Murgia Natura 2000 site. This area is currently being studied and used as a test site in BIO_SOS. We focus on mathematical models of metapopulation dynamics. The rationale for this selection of analytical approach is that the extension and vegetation type of the Alta Murgia site is not suited for hosting a viable and stable population of predators. Thus, any conservation policy for similar cases has to be established at a metapopulation level. Metapopulation dynamics, i.e. the dynamics of a "population of populations", represent an effective tool for investigating the dispersal of species population in fragmented habitat. The predator-prey community is divided in smaller populations living in sub-domains (patches) surrounded by a non-habitat part of the landscape. The communication among the patches occurs through corridors. Such a scenario is common to landscapes subject to anthropic pressures. Mathematical models and methods, developed for studying the dynamics of cyclic populations in fragmented habitats may produce qualitative results to support management decisions. This part of the deliverable deals with a new mathematical model for analyzing the effect of corridor size on the predator-prey dynamics in a metapopulation framework. It represents a preliminary study to be further developed by integrating quantitative data measurements from the field in order to set the proper model parameters for the case at hand.

2. Introduction

Biodiversity conservation policies require procedures for observing, controlling, surveillance and detection of changes as well as for building scenarios to simulate feasible rehabilitation actions for degraded landscapes. Among the factors and processes to be monitored to ensure the appropriate edaphic environment for conservation of endangered habitats, a key role is played by the interaction of climate with soil.

The surface hydrology of a landscape (i.e. rainfall, infiltration, runoff, erosion, plant growth and nutrient cycling) strongly contributes to determining the state of health of its ecosystem, when considering the landscape as an organized system where each part functionally interacts/cooperates with other components to collect, store and distribute resources for supporting life.

The description, the analysis and the interpretation of ecosystem functions (i.e., the processes that occur in it, their consequences, the ecosystem degree of health, the drivers and pressures that are generated outside but affect the ecosystem state continuously or in pulses), represent the core of the Landscape Function Analysis (LFA, Ludwig et al.[1998]). LFA is a monitoring procedure, embedded in a conceptual approach, that exploits rapidly acquired field-assessed indicators to assess the biogeochemical functioning of landscapes at the hillslope scale¹. An objective of the BIO_SOS project, as summarized in WP6, Task 6.3, is to develop a similar approach to tackle ecosystem functions on project sites selected by ranked set sampling design in connection to well proven standard methods of vegetation surveys. LFA is a monitoring procedure that assesses how well an ecosystem works as a biogeochemical system, using simple indicators. It is intended for repeated measurements to present the data as a time series (trajectory). It includes evaluation of ecosystem fragmentation, and connectivity between patches of similar niches or ecosystem sub-unit can be easily assessed using the measurements suggested by the Ludwig et al [1998]. It has been applied to a wide variety of landscape types and land uses. This approach can be merged with the recently developed approaches for sediment and water runoff-runon connectivity. The concept of connectivity as understood in this task is relevant to hydrological connectivity as, despite a considerable number of studies that use or address the concept of connectivity, there is no broad consensus on its definition. This may result from the fact that connectivity studies are often case/species-specific, limited to particular land units and scales, and focus on the flux of different elements like water, sediment and fauna. Moreover an evident knowledge gap in the establishment of quantitative measures to evaluate factors such as frictions met along specific paths by the animal, water, sediment has further diluted the connectivity property of an environment and the possibility to estimate it quantitatively. Here connectivity for subject X is intended as the integrated assessment of elements favouring a smooth passage of X from a site A to another site B in the real 3D landscape where non anthropic and anthropic processes interact. Each single pixel can be characterized by a value of friction exerted against the passing through of X. The spatial distribution of these friction values can be transformed into a probability for X to move from A to B (which can differ from the probability for a successful move of X from B to A).

The activity included: a) In-field campaigns for quantitative variable measurement; b) integration with satellite derived products; c) assessing hydrological and sediment connectivity

1

3. Part I. Landscape, plants, landslides and erosion model (LANDPLANER)

A new landscape, plants, landslides and erosion model has been developed with the aim of performing the ecosystem assessment for the study sites of the BIO_SOS project. This model is based on the Landscape Function Analysis (LFA) approach, similar to that proposed by Ludwig et al. [1998], in connection to standard methods of vegetation surveys. It is a model that can work at its best using VHR satellite images and algorithms to spatialize data following indices of vegetation density within the same land use class. This will become evident during the description of the model. We also took the mean annual sediment connectivity model by Borselli et al. (2008) as a model to imitate for getting input-data tables already existing, so to use already existing knowledge without re-inventing new tables. This choice of using parameters, whose values have already been determined, may be seen as a limit but this actually makes the work feasible within the BIO_SOS time table as we only have to focus on the physico-mathematical relationships without having to measure ad hoc parameters in a myriad of conditions.

LANDPLANER builds on a series of pre-existing models and software tools:

- Grass GIS and its r.watershed functions (© GRASS Development Team, 1998-2013)
- R software (© The R Foundation for Statistical Computing) where most of the array computation is done.

The models here used are:

1. NRCS Runoff Curve Number method
2. EUROSEM2013 runoff-erosion model

The item 1 is deeply embedded into the model while item 2 is used for checking results and validate trends. The choice of using R is simply due to that fact that most of the variables are multi-dimension tables and matrices. Obviously spatially distributing landscape characteristics means working in a particular environment such as GRASS GIS but any GIS software would do. More specifically the watershed procedures, originally developed by Mitasova and her team, includes a series of tools which are extremely useful: r.watershed (watershed basin analysis program), i.e. such as the single flow direction calculation algorithm (D8), the flow accumulation calculation working also with the sink (depression) algorithm on; and r.slope.aspect, to generate the slope map.

3.1 Effects of roads: a new tool developed in GRASS (r.sim.road)

As roads and other linear structures often are averaged in DTMs of the cell size larger or equal to the road width, it was decided to modify the DTM elevation values corresponding to cells belonging to roads in order reproduce road effects on flow direction and accumulation. Hence, a special tool had been developed in GRASS GIS (r.sim.road) for dealing with elevation map modification linked to the presence of roads in a DTM too coarse for the road to be identified as a landscape feature. In particular, the original slope is re-profiled (either or both dug and/or raised): the operation involves three pixel transversal to the road trajectory, the middle one with the road in it. The three cells are brought to the same elevation as the central one, hence the road is flat in the direction transversal to the road while the cells at the boundaries become steeper. When the original slope is below a threshold the three cells are all raised, constituting a small impermeable dam. The two cases are shown in Figure I.1.

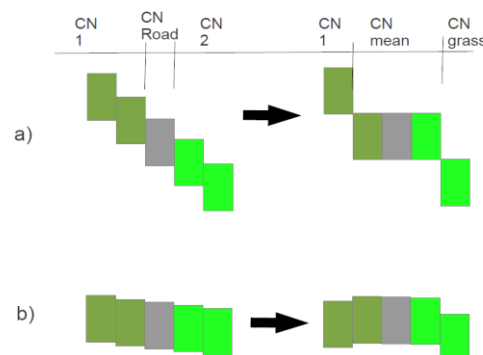


Figure I.1 Cell elevation modification to include the effect of roads on flow direction: the cross section depicts the road surrounded by 4 pixels with two different land uses. Case b) is applied when slope gradient is low. Other corrections are possible. The modification also includes a change in CN attribution (see text).

3.2 NRCS Curve number method

The CN method has simple but rich tables for transforming land use classes into data useful for daily runoff calculation. It has limited need for information about rainfall, only utilizing information about daily rainfall. It does not involve complex hydrology computations, 3zhence at the end the tool remains easy to use.

The basic equation is:

$$Q = \frac{(P - \lambda S_{\lambda})^2}{P + (1 - \lambda) S_{\lambda}} \quad (1)$$

where Q is daily runoff (mm), P is the corresponding daily rainfall (mm), S_{λ} (mm) is the maximum potential loss to runoff, and λ is the fraction of S_{λ} which represents the initial abstraction.

S_{λ} is a storage index, a measure of the catchment hydrological response. It is calculated once the Curve Number (CN) is defined using tables describing various field conditions where land use and hydrologic soil groups are the two main inputs. The basic equation was first derived for $\lambda=0.2$ i.e.:

$$S_{0.20} = 25.4 \left[\frac{1000}{CN} - 10 \right] \quad (2)$$

More recent studies suggest a much lower value for λ : Hawkins et al. (2009) proposed $\lambda=0.05$, while Mishra et al. (2003) suggest $\lambda=0.00$. We will follow Hawkins et al. (2009)'s suggestions. Accordingly, $S_{0.20}$ was transformed into $S_{0.05}$ using the equation (where both S-values are expressed in mm):

$$S_{0.05} = 0.819 S_{0.20}^{1.15} \quad (3)$$

CN values are given in 2-entries tables (e.g. see. Table I.1) and selected following the hydrologic soil group and the land use.

This type of choice is in agreement with the approach followed by Borselli et al. (2008) for sediment connectivity: they used the C factor of RUSLE (Renard et al. 2001) because this factor C summarizes the effect of different land uses and management on soil erosion, exactly as the CN-values in the CN method. Then we opted for introducing a difference with respect the standard use of the CN in hydrology. This modification is introduced following the LFA approach proposed by Ludwig et al. [1998]. To understand the originality of our approach let us compare it with its standard version. The main issue is that the standard runoff CN model is lumped and a catchment is represented by one single value of CN which represents the weighted average of the CN values of the land uses present in the studied basin. This single value is then used to transform rainfall into daily runoff (eq.1). Daily runoff is a measure of the water exiting the catchment and nothing is said about the behaviour inside: the catchment is not described in its internal diversity. The cell A of Figure I.2 represents either a cell or a basin: no description of what occur inside the catchment is given. We proceeded in a different way by attributing to each pixel its own CN-value. This change means that the cells on a divide (cell A of Figure I.2) uses only rainfall as input while all the other cells (cell B of Figure I.2) receives both rain and runoff from upstream pixels. Rain and runoff are summed and substituted for rain in eq.1. In other terms the general form of eq.1 becomes:

$$Q_{off} = \frac{(P + \sum Q_{on} - \lambda S)^2}{P + \sum Q_{on} + (1 - \lambda)S}$$

(4)

Table I.1 Example of Curve number tables (NRCS, 2004) for arid and semi-arid zones.

Hydrologic Soil Group					
LAND USE	Hydr. Cond.	A	B	C	D
Herbaceous—mixture of grass, weeds and low-growing brush, with brush the minor element	Poor		80	87	93
	Fair		71	81	89
	Good		62	74	85
Oak-aspen—mountain brush mixture of oak brush, aspen, mountain mahogany, bitter brush, maple, and other brush	Poor		66	74	79
	Fair		48	57	63
	Good		30	41	48
Pinyon-juniper—pinyon, juniper, or both; grass understory	Poor		75	85	89
	Fair		58	73	80
	Good		41	61	71
Sage-grass—sage with an understory of grass	Poor		67	80	85
	Fair		51	63	70
	Good		35	47	55
Desert shrub—major plants include saltbush, greasewood, creosote bush, blackbrush, bursage, palo verde, mesquite, and cactus	Poor	63	77	85	88
	Fair	55	72	81	86
	Good	49	68	79	84

If we compare runoff from the catchment and rainfall and calculate the catchment CN we observe the same types of trends that are observed when runoff is measured in real catchments: this “strange” catchment behaviour can be explained by the simple spatial variation of CN values, i.e. the spatial variation of catchment characteristics relevant for runoff production. This unexpected result is a fact corroborating our choice and explaining the asymptotic-behaviour correction to CN recently suggested by Hawkins et al. (2010).

The similarity of this approach to Ludwig et al. (1998) is that in both cases flow lines are followed and every x meters (in the LFA approach) or every cell (in our approach) the vegetation-landuse in LFA approach, CN-values based on vegetation-landuse (and NDVI variation within each landuse) in our approach, are defined. Eq.4 summarizes mathematically our approach.

This approach allows us to calculate daily runoff at each cell within our catchment. Furthermore, we can also calculate the amount of water infiltrated in each cell. This is important for calculating local water availability as water stored into the soil and available to plants: while at the divide² the amount of water infiltration is a fraction of rainfall, in some downslope cells the amount of water infiltration can be higher than the amount received as rainfall because of runoff harvesting. Knowing how water is distributed in the catchment can help in managing habitat patches especially where water is a limiting factor, either because of scarcity or because of abundance. This also

²

represents a significant methodological advance in respect to what can be obtained adopting the standard use of CN.

Then we proceeded to attribute a CN-values to the pixels attributed to roads. The roads, especially after the DTM treatment described before while presenting `r.sim.road`, need their own CN values which cannot depend only on the particular road characteristics such as dirt road or paved road, because there are 3 cells involved and for narrow roads and large pixels sides the road does not even fill one full cell. So the value for the three cells is derived from the weighted average of the CNs of the land use at one side of the road, the land use at the other side and the CN of the road itself. The size of the road versus the size of the three pixels provides the weighing factor used for calculating the average CN. In order to compute the weighted average automatically, roads are subdivided into 5 categories: field tracks (narrow, more or less at the same elevation of the surrounding terrain, dirt roads), municipal roads (larger than field tracks, but still narrow, usually paved), provincial roads (intermediate size, about 10m large, paved and with ditches), national roads (15 m large, paved, with ditches), highways (20-30m large: to be checked whether the DTM has already made them visible).

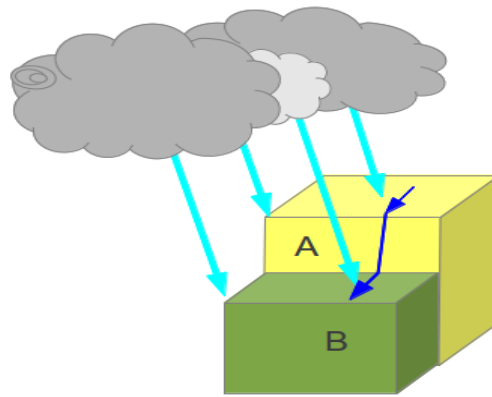


Figure I.2 While in cell A only rainfall is the input, cell B receives both rain and runoff. CN method uses an average CN for the whole basin, our model uses different CN-values at each cell. Each cell then receive both runoff and rain and uses both to calculate what is exported as runoff towards the downslope cell.

In order to evaluate the degree of reliability of the model, we compared it with simulations made using the EUROSEM2013 model which is an event model derived from KINEROS 1 and developed through a group of European funded projects (EUROSEM, SPIE, MWISED, RECONDES, DESIRE), which is still used today and kept updated: it is presently undergoing a further development to include hydrophobic behaviour and gully generation. The comparison between the two models is still ongoing.

Ephemeral gully generation is an important part to address for a proper landscape management because the rainfall in which gully are generated produces high amount of sediment and modify runoff concentration time which is critical for peak runoff. The presence of a gully also changes the pattern of infiltration and may sever areas from runoff harvesting. Areas where ephemeral gullies tend to form are ideal to be used as grassed waterways, increasing the protected corridors between patches of protected areas.

3.3 A theoretical approach to describe gully head development by runoff

In the 1970s, Patton and Schumm (1975) and Begin and Schumm (1979) began modelling gully erosion as a threshold process, and suggested that an equation defining such threshold could be derived from the fact that concentrated overland flow should produce flow shear stresses in excess of a critical value to erode a gully channel. This approach was further developed by Montgomery and Dietrich (1994). The starting point is that the flow shear stress produced by runoff must exceed a threshold soil shear resistance. This leads to the following inequality:

$$sA^b \geq k \quad \text{or} \quad s \geq kA^{-b} \quad (5)$$

Figure I.3 shows example of trends between catchment area upslope of the gully head and the slope (sinus) around the gully head (based on a literature survey). The threshold for gully head to develop is the one reported in Figure I.3. It can be noted that trends are scattered but they develop almost parallel to each other. Hence the exponent b is a constant ($b=0.38$). Under these circumstances it is possible to estimate k (i.e. the value of slope when the area of the catchment above the gully-head is 1 ha): Torri and Poesen (2013, submitted) shows that k depends linearly on the storage parameter of the runoff CN method. Hence, we modified equation (5) into equation (6), where γ is the local gradient and A is the area of the upslope catchment draining into the gully head while $S_{0.05}$ is calculated from CN through equations 2 and 3:

$$\sin(\gamma) \geq 0.73 ce^{1.3RFC} (0.00124 S_{0.05} - 0.037) A^{-0.38} \quad (6)$$

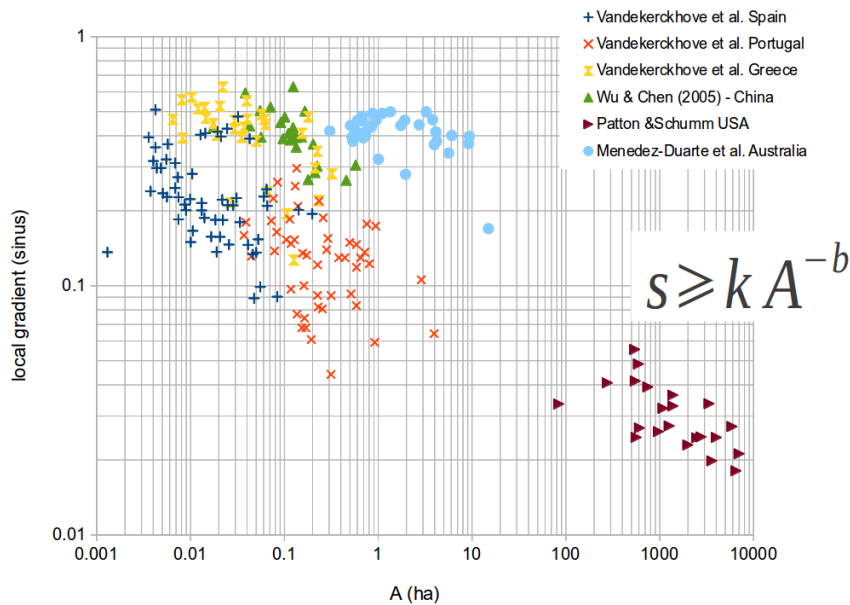


Figure I.3 Relationship between local gradient nearby the gully head and the catchment area draining into the gully head. Data comes from the following papers: Vandekerckhove et al. (2000), Wu and Chen (2005), Patton and Schum (1975), Menendez-Duarte et al. (2007).

The model here described (LANDPLANER) is based on the above described background and original developments. It can be used for scenario analysis to decide how to deal with pressure derived from water and sediment requirement and control. It is a tool to examine water and sediment fluxes, their connectivity and their interaction with the general land management.

3.4 LANDPLANER description

LANDPLANER (Landscape, Plants, Landslide and Erosion) is a model designed to describe the dynamic response of slopes (or basins) under different changing scenarios. Scenarios include: (i) changes of meteorological factors (i.e. rainfall) or more generally of climatic conditions, (ii) changes of vegetation or land-use, (iii) changes of slope morphology (e.g. close to roads). Both natural and anthropic changes scenarios can be analysed by the model.

The input data (maps) which are used by the LANDPLANER are:

- ⤴ DTM
- ⤴ modification of DTM in order to describe the road effects
- ⤴ flow direction
- ⤴ flow accumulation
- ⤴ sinks
- ⤴ soil (or lithology) map
- ⤴ landuse
- ⤴ derived map of CN and a map of soil resistance
- ⤴ map(s) of precipitation

Table I.1 *List of the variables with corresponding description*

Variables	Description
acc_abs.asc	Accumulation value (number of cell identifying the upslope contributing area draining in each cell)
acp_hor_h_xxx.asc	Horizontal acceptance of the horizon xxx
acp_hor_v_xxx.asc	Vertical acceptance of the horizon xxx
ba.asc	Basin codes (integer number identifying pixels pertaining to the same hydrological basin)
dd_abs.asc	Drainage direction (calculated with Single Flow Direction or D8 method)
dep.asc	Depositions index (given by the difference between e _{pot} and e)
e.asc	Erosion index (expressing the expected erosion impact)
ecc_hor_xxx.asc	Excess water of the horizon xxx (excess of water in a cell that exceed the total cell storage)
ecc_hor_h_xxx.asc	Horizontal excess water of the horizon xxx (excess of water in a cell that exceed horizontal acceptance)
ecc_hor_v_xxx.asc	Vertical excess water of the horizon xxx (excess of water in a cell that exceed vertical acceptance)
edp.asc	Cells where deposition expected (0 or 1 derived from topographic threshold, Erosion Deposition Points)
eout.asc	Erosion index (exiting from each cell)
epot.asc	Potential erosion index (in each cell)
esp.asc	Cells where erosion is expected (0 or 1 derived from topographic threshold, Erosion Starting Points)
infil.asc	Surface water infiltrating in each cell
qd.asc	Total runoff (in each cell)
qd_hor_xxx.asc	Total runoff of the horizon xxx (water exiting from each cell of the horizon)
qd_norm.asc	Normalized runoff (given by the ratio between qd and the contributing area)
qdout.asc	Total runoff (exiting from each cell)
ra_col.asc	Index of column of destination cell (derived from drainage direction)
ra_row.asc	Index of rows of destination cell (derived from drainage direction)
residual_flux_bidimentional.asc	Residual flux below the deepest soil horizon (bidimensional infiltration model)
residual_flux_simplified.asc	Residual flux below the deepest soil horizon (unidimensional infiltration model)

sl_dp.asc	Slope difference between origin and destination cell (used in calculation of edp)
stor_hor_xxx.asc	Total water storage of the horizon xxx
stor_hor_in_xxx.asc	Initial water storage of the horizon xxx
stor_hor_pot_mac_xxx.asc	Macro-porosity water storage of the horizon xxx
stor_hor_pot_mic_xxx.asc	Micro-porosity water storage of the horizon xxx

LANDPLANER outputs consist of maps in ascii format relative to the different hydro-geological, hydrological, geomorphological, land-use and vegetation variables. Outputs can be relative to the surface or to different soil horizon denoted with “hor”. Since the model can deal with different soil horizons, the outputs of the infiltration model are denoted with the suffix xxx representing the different horizon considered in the analysis.

The most important LANDPLANER outputs are:

- ⌘ runoff map (litre in each pixel) and runoff intensity map (mm per pixel, which represent the mm of runoff intensity averaged over the catchment area drained at the pixel)
- ⌘ infiltrated water map (mm infiltrated in each pixel)
- ⌘ erosion/deposition map (total and mass per unit of surface)

items 1 and 2 are already values while items 3 necessitate of a validation and a scaling which will be done using simulation with the EUROSEM2013 model which is an event model derived from KINEROS I and developed through many European funded projects (EUROSEM, SPIE, MWISED, RECONDES, DESIRE) presently undergoing a further development to include properly hydrophobic behaviour and gull generation.

Still to be added to the erosion part is the generation of ephemeral gullies in cropland and in degraded rangeland. The equations to put into the model are ready but still not fully implemented.

3.5 Examples of scenario analyses

At present LANDPLANER can be used in scenario analyses. For this we have chosen the catchment of the karst sink “pulo di Altamura” in the Murgea Alta test site. The following is shown with particular reference to infiltration, runoff, and a hypothesis of improved “pulo” protection. This is only an exercise and does not necessarily describe the real conditions at the pulo because input data need some further field evaluations and tuning. We have built one scenario based on the actual spatial distribution of land uses and tested it under autumn and spring conditions. Then, we have changed land use in a small area around the pulo, as if to protect it from pollutants carried by runoff from agricultural fields. Just to stress the situation we have supposed a broadleaved wood with a rich bush undergrowth. This guarantees a decreased runoff and an intense sedimentation before water can reach the pulo. It also causes runoff to be largely infiltrated. Infiltration water will eventually reach the water table after having left most of the pollutants in the soil-rocks during the slow motion downward. If the scenario is compared with another scenario based on a different type of vegetation, it will further enable assessment of the minimum effort required for maximum (or sufficient) returns. Then we have also examined another scenario where we simulated after-fire condition on an internal slope of the pulo.

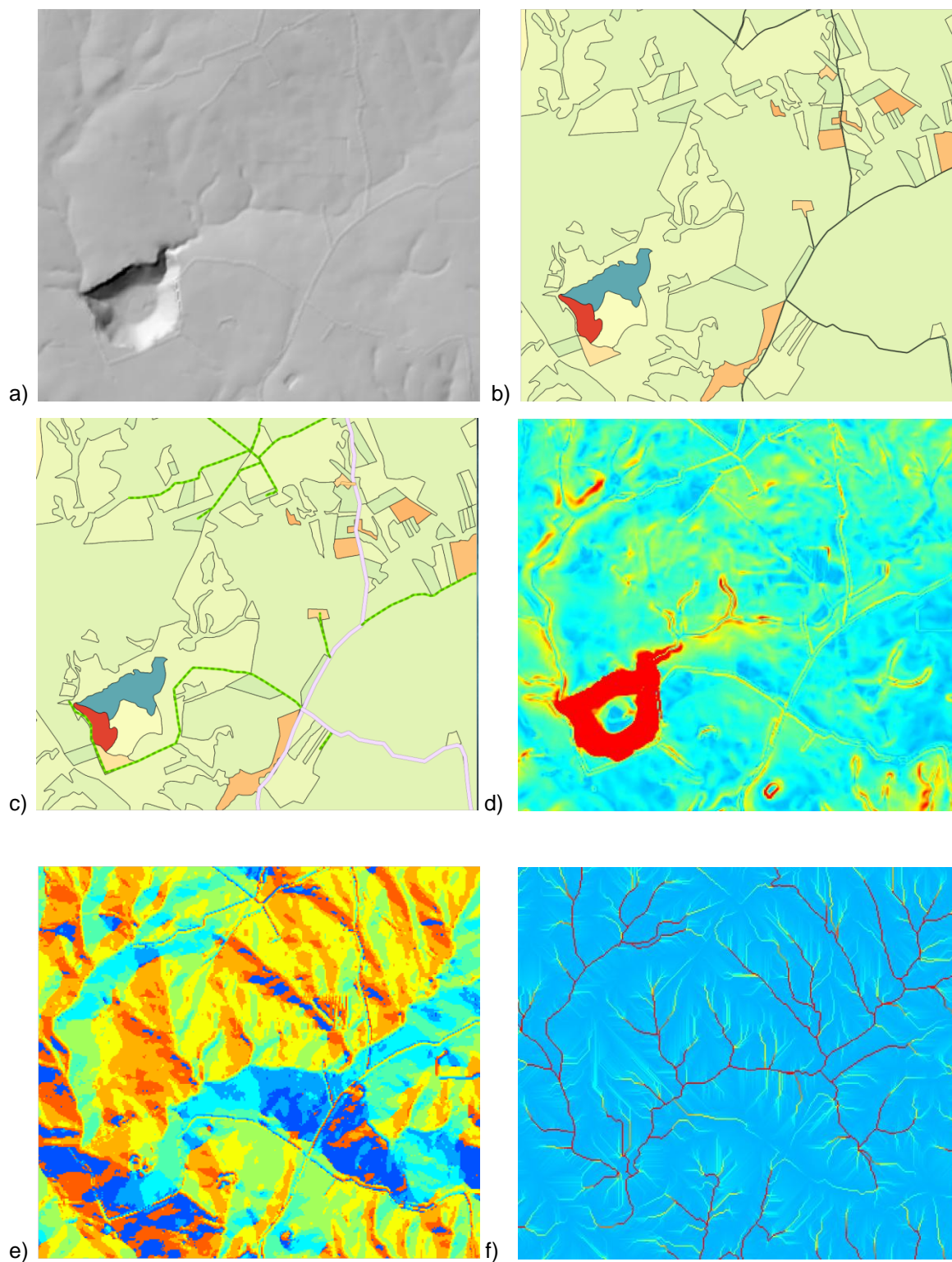


Figure I.4: some input map of LANDPLANER: a) DTM, b) Land use , c) Roads, d) slope; e) drainage directions (D8); and f) flow accumulation.

Figure I.4e shows the flow accumulation in presence of roads. Figure I.5 shows the differences that can be observed with and without the use of `r.sim.road`, which introduces the effect of roads on flow direction.

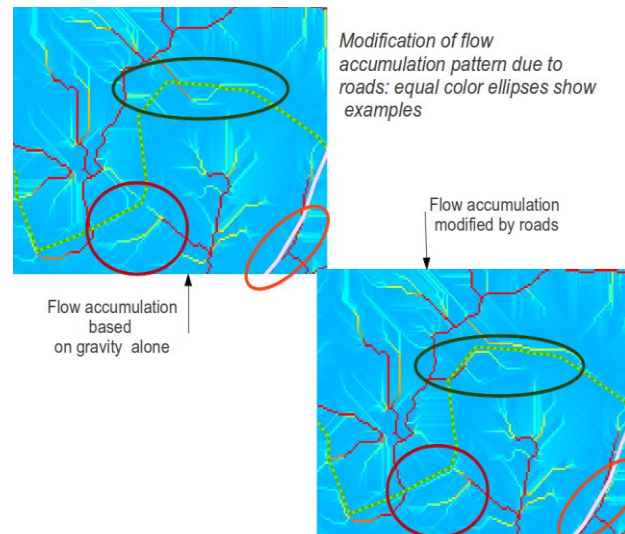


Figure I.5: Flow accumulation is re-directed by roads: this can have positive as well as negative effects: where concentration is enhanced there are larger probability that a gully develop; where runoff is captured and diverted can cause local plant damage due to lack of water availability in the soil.

The example discussed here also shows that the combined effect of a coarse DTM and of any modification (such as the one by `r.sim.road`) can cause an unrealistic road effect as indicated in Figure I.6.

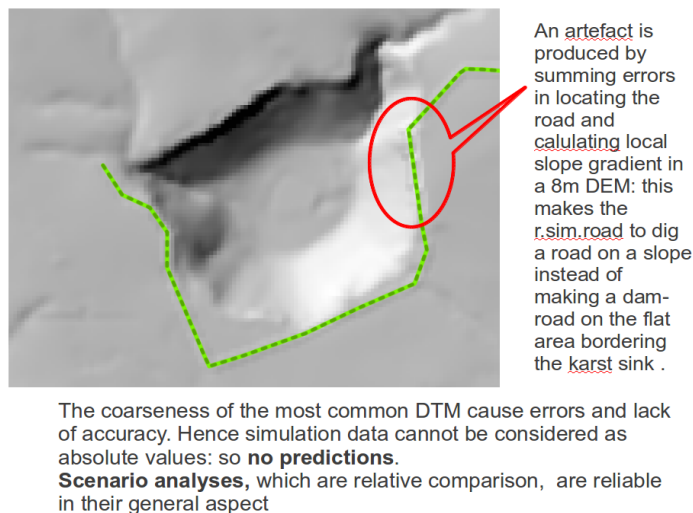


Figure I.6: example of mismatch between representation and reality: the road runs only in flat area surrounding the pulo.

An example of CN map, representing a springtime situation is shown in Figure I.7. Here CN values are constant inside each landuse: the spatial differences that can be visualized using NDVI have not been calculated.



Figure I.7: Curve number distribution around the pulo: CN increases from blue to red. Roads and farms are visible for their red colour.

Now a map of daily precipitation can be fed to LANDPLANER. At present we are still working out bugs which can be detected more easily if rainfall spatial distribution does not add further sources of variation. So only single values of daily rainfall are fed to the model. If we use a daily runoff corresponding to a rare event (80mm) we obtain the runoff map shown in Figure I.8 (autumn conditions). If we want to understand differences of runoff distribution in spring and autumn a difference map can be calculated for the same rainfall amount for the two situations. An example of such a map is shown in Figure I.9. It is interesting to note that in our approximate representation the amount of water reaching the pulo directly as surface runoff is not substantially different in the two seasons, which is partly due to the fact that we did not change vegetation characteristics between autumn and spring inside the pulo. This also partly depends on the relative isolation of the pulo from the surrounding area, as most of the overland flow water infiltration takes place scloser to the pulo lowland.

In order to examine the extent to which the pulo is isolated from external overland flow, we can decrease the CN of the area around the pulo, e.g. transforming the grassland into a wooded area as indicated in Figure I.10a (electric blue in the small frame showing decreased CN-value). Figure I.10b is the difference between the spring runoff map and the modified-CN runoff. The area inside the pulo is filled with zero-runoff values. The increase in isolation has not caused any change in the area encircled by it, confirming the lack of connection of the pulo to surrounding runoff source areas.

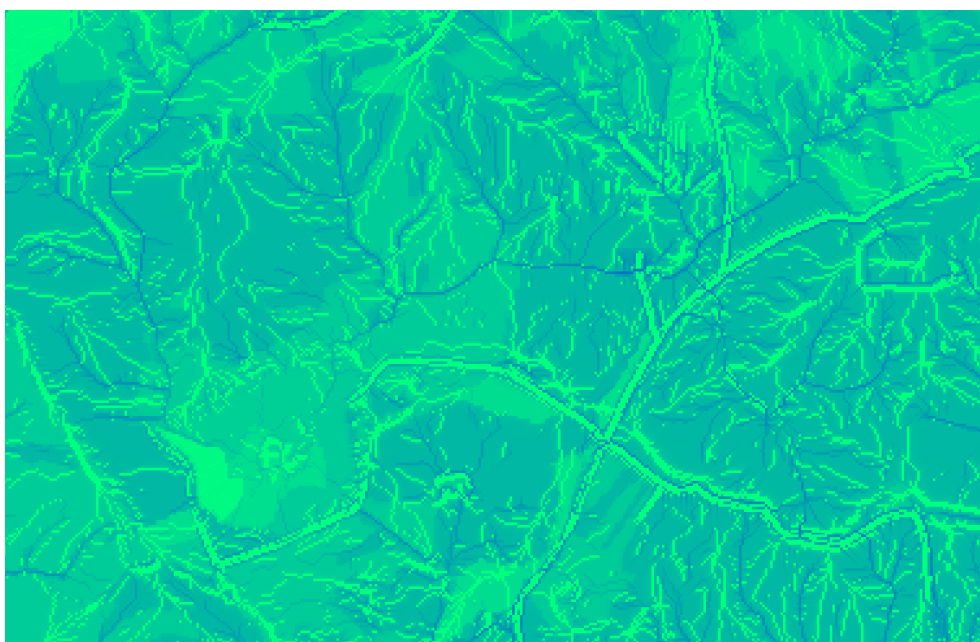


Figure I.8 *Runoff map for an autumn rain of 80 mm in a day.*

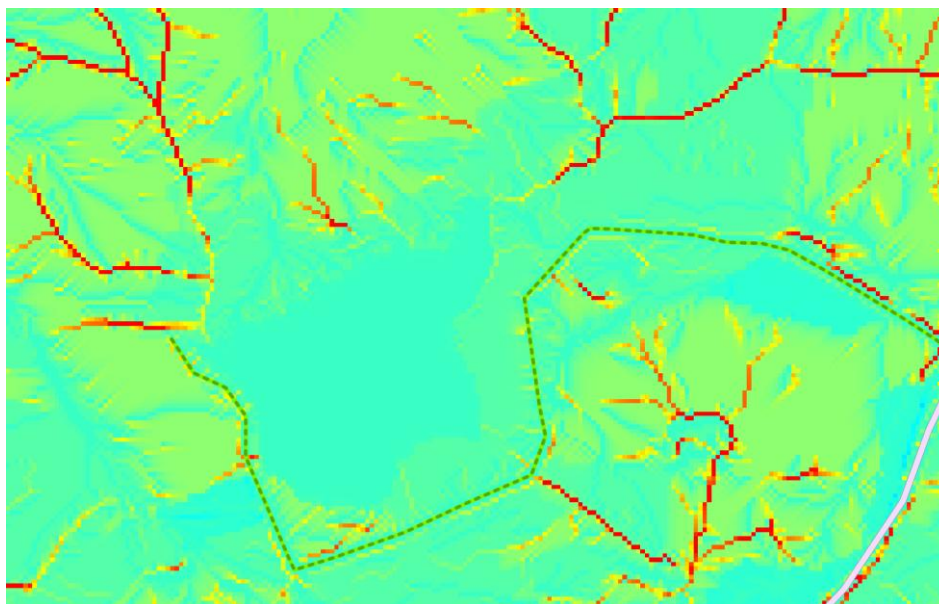
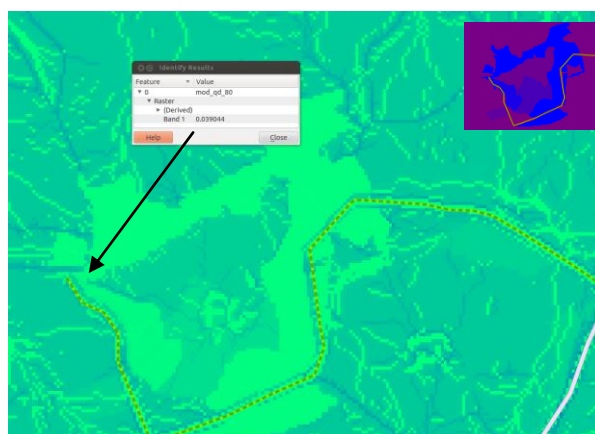
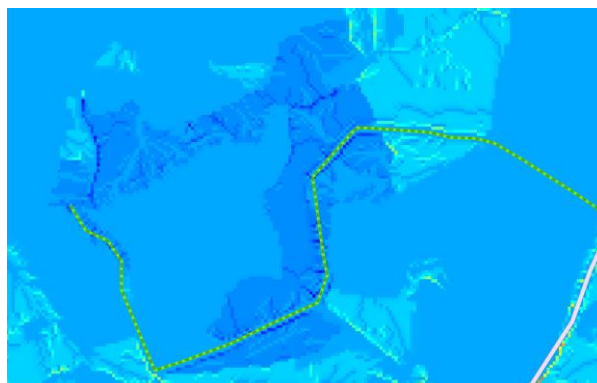


Figure I.9 *Runoff differences between two 80mm daily rainfall in autumn and spring. Red cell indicates a larger autumn runoff exceeding spring runoff of up to 250 l. Pale cyan, as inside the pulo, is an almost zero value*



a)



b)

Figure I.10 *a) The runoff map (80 mm, spring rainfall) shows that runoff values where the arrow points are very low, supporting overland flow disconnection (the small frame in the upper right corner shows in blue the area of*

changed CN); b) the map showing the differences in runoff between the spring original and modified scenario clearly shows that runoff inside the pulo does not change increasing the pulo isolation (the azure colour inside the pulo indicate zero change).

Effects of destructive event such as a fire inside the pulo, with burning on the northern slope, shows that the same 80mm event can become quite damaging inside if it occurs after the fire (mainly with no smaller rainfall in between to reduce acquired hydrorepellency). This highlights the risk of losing soil cover and damaging the seed bank, thereby reducing the chances of vegetation recovery (Figure I.11).

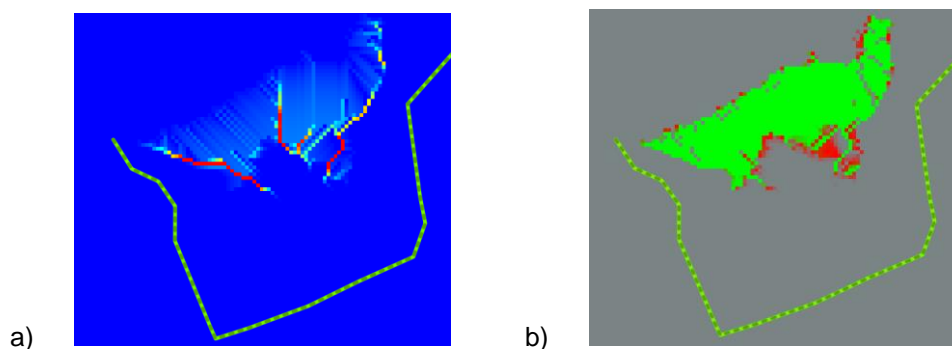


Figure I.11 a) Differences in runoff due to a fire in the northern slope of the pulo; b) difference in erosion. The blue (a) and grey (b) colored part indicates no variation between the two scenarios. In both cases red indicates maximum difference.

3.6 Part I. Conclusions

LANDPLANER is part of EODHAM in which it can be better integrated or otherwise left independent following what will be considered the best solution. This model requires inputs which are produced and handled by EODHAM, hence it can run downstream most of the EODHAM products. Hence reference simulations can run on an updated landscape and evidence the presence of changes from which an educated user can deduce whether some of the pressures on the protected sites are increasing.

It cannot be used by non-specialists yet as it needs a simplified procedure and a user manual. It can be used in scenarios more complicated than the ones here discussed. It can also help to better understand the impact of various landscape elements, such as the stone walls that subdivide fields and pastures in many part of Europe, on hydrology and landscape health, provided that good and usable maps of these structures exist. Hence, LANDPLANER is an instrument for assessing the effects of planned actions on water and sediment distribution in the landscape and for deciding the effect that potential management responses and actions could produce.

4. Part II. Metapopulation dynamics: the effect of corridor size in spatially explicit/implicit models

Among the many and different ecological landscape modifications induced by human pressures, habitat fragmentation and its effect on biodiversity has a major role in landscape modeling. In order to study how this spatial process affects cyclic population dynamics, explicit metapopulation models described by reaction-diffusion partial differential equations are here considered. Indeed, implicit metapopulation models described by ordinary differential equations, having no spatial dimension, cannot take into account landscape features such as size and heterogeneity of the domains, as well as migration corridor sizes. However, spatially explicit models which show the importance of landscape context in metapopulation dynamics, are computationally heavy and do not allow any theoretical study of the solution behavior. In this paper we focus on the effects of migration corridor size reduction on cyclic population dynamics by means of classical spatially explicit models and we propose new spatially implicit ones which inherit the information of spatial explicit models from which they are deduced. A numerical comparison between the two approaches confirms that the proposed implicit model captures the qualitative features of the explicit one and may reveal as an effective tool for a further theoretical analysis able to provide some predictive biological information. Finally, a comparison among the answers of four classical models found in the literature to both patches and corridor entrance size variations show that, for given values of the parameters, different dynamics may arise: this suggests that the correct choice of the model as well as the estimation of its parameters will be crucial for a realistic modeling study of predator-prey pairs

4.1 Background

The ecological effects of human activities induce different changes in natural habitats. Habitat fragmentation is one of the classical consequences of human population growth: indeed, given human population activities and urban sprawl, habitats are often fragmented into patches connected via migration corridors set in non habitat portions of the landscape (Fahrig, 2003). For cyclic predator-prey population dynamics, on which we focus our attention, experimental and theoretical results suggest that the subdivision of the same amount of habitat into smaller pieces may also provide positive effects on their stability (Huffaker 1958, Baggio et al. 2011); however the increasing reduction of the size of migration corridors abates the number of the individuals that are able to migrate from a patch to another and species are confined in more and more isolated patches. When increasing fragmentation produces patches too small to sustain local populations, the worst consequence of the reduction of the size of migration corridor is the extinction of the species. This motives us to consider the effects of such reduction on the permanence or the extinction of cyclic populations living in a fragmented habitat, such as the wolf - wild boar pair which populates the Italian Alta Murgia Natura 2000 site, whose extension and vegetation type is not suited for hosting a viable and stable population of predators. Any conservation policy for similar cases has to be established at a metapopulation level. This area is currently being studied and used as a test site in BIO_SOS.

Metapopulation dynamics, i.e. the dynamics of a "population of populations" (Levins 1969), represent an effective tool for investigating the dispersal of species population in fragmented habitat. As concerns ecological cyclic processes, starting with the Jansen's paper (Jansen 2001), mathematical models describing dynamics in patchy landscapes are generally spatially implicit, meaning that they have no spatial dimension and all patches are accessible via dimensionless corridors. As a consequence, the models are described by means of ordinary differential equations coupled through diffusion coefficients that model the migration of species from a patch to another. Lotka-Volterra (LV) systems (Okubo and Levin 2001) as well as its modifications like Rosenzweig-MacArthur (RM) (Rosenzweig and MacArthur 1963), May (May 1974) and Variable Territory (VT) (Turchin and Batzli 2001) are the most widely used differential equations considered in this context.

However, in recent years, the consideration of spatial processes in ecological systems has been growing and spatially explicit modeling has revealed to be more effective for the ecological understanding of such kind of phenomena (Conroy et al. 1995, Dunning et al. 1996, South 1999, Turner et al. 1995).

As concerns cyclic population dynamics, a numerical study provided (Strohm and Tyson 2001) investigates the effects of habitat fragmentation through spatially explicit models i.e. models which take into account the spatial dimension. In that paper the authors define as 'bad' patches that parts of the habitat where migration of predator and prey occurs and prey population cannot grow. The predator and prey migration is modelled through transport terms acting only in the 'bad' patches which are included in two coupled diffusive PDE equations that describe the population dynamics in the whole domain Ω (see the illustrative example in Figure II.1). Consequently, the authors depart from a metapopulation dynamics approach where the domain Ω is considered as fragmented in more smaller domains Ω_i (that correspond to the 'good patches' of the previous approach) and migration corridors are set

in non habitat portions of the landscape i.e. outside the domains Ω_i . In this case two coupled reaction-diffusion equations describe the dynamics in each domain Ω_i and they are linked by migration diffusion terms occurring only at corridor entrance positions (see Figure II.2). In this framework, some numerical results based on a two-dimensional spatially extended predator-prey model can be found in Garvie and Golinski 2010.

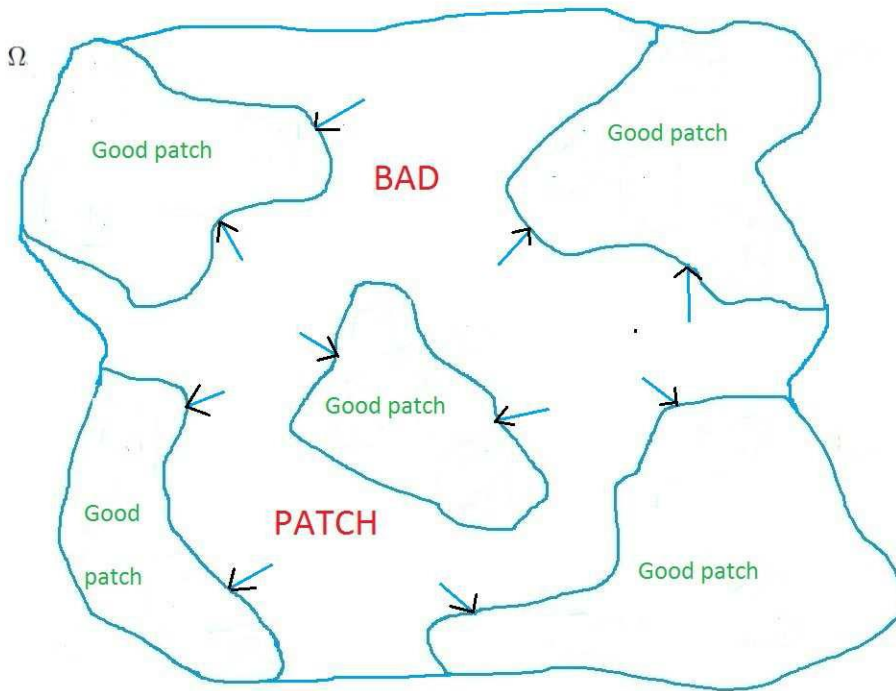


Figure II.1 An illustration of a generic five 'good patches' two-dimensional single-population spatially explicit model; migration occurs in the habitat's bad patch inside the domain Ω towards good patches (for details see Strohm and Tyson 2001).

Unfortunately, the integration of the spatial dimension is difficult and expensive both practically to parametrize spatially-explicit models (Urban and Keitt 2001) and numerically to provide accurate solutions (Garvie and Golinski 2010). Furthermore, it leads sometimes to qualitatively similar predictions found by alternative approaches as, for example, the graph theory which has minimal data requirements and efficient algorithms (Baggio et al. 2011, Urban and Keitt 2001). As concerns cyclic population dynamics, by reducing spatially explicit models into spatially implicit equivalent ones it is possible to capture the main features of the spatially explicit models and use standard mathematical tools to study the solution behaviour (Strohm and Tyson 2011).

By following a metapopulation approach similar to the one provided in (Garvie and Golinski 2010), we firstly numerically investigate the answer of the spatially explicit reaction-diffusion RM model to the variation of corridor entrance size; the results are then compared with the ones provided by a new reduced implicit model where the spatial dependence is taken into account via relationships which link growth and death rates of prey and predators with the sizes of each patch and of the corridor entrances.

In so doing, we were motivated by the results in (Strohm and Tyson 2011); indeed the implicit model, described by ordinary differential equations, may reveal an effective tool for a theoretical investigation of the effects of both the reduction of patches and migration corridor entrance sizes that is the aspect of the fragmentation process on which this paper is focused. Finally, for supporting the choice among the different models given in the literature for simulations of the predator-prey dynamics populating "Natura 2000" sites of interest for the BIO_SOS project, a preliminary numerical comparison among the different answers obtained by considering different models to the corridor entrance size variation is also provided.

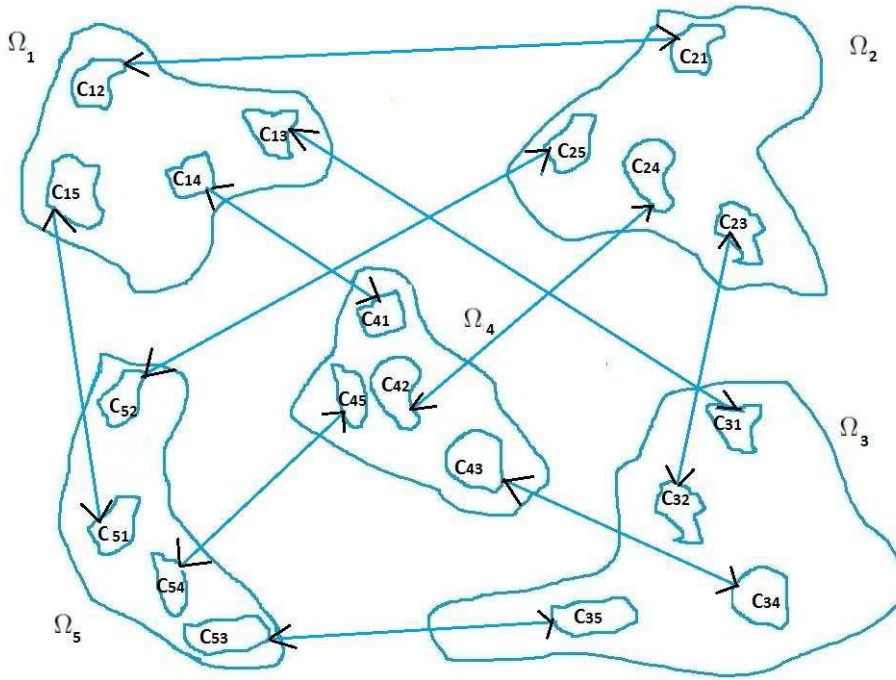


Figure II.2 An illustration of a generic five-domains two-dimensional metapopulation spatially explicit model; migration occurs through corridor entrances $C_{ij}=C_{ji}$ in non habitat part outside the domains Ω_i , $i,j=1,\dots,5$.

4.2 The spatially explicit model

In this section we introduce the most general metapopulation model as composed of N patches where the movement of each prey-predator subpopulation is modeled by a random Fickian diffusion and a reaction term:

$$\begin{aligned} \frac{\partial n_i}{\partial t} &= D_i^{(n)} \Delta n_i + f(n_i, p_i) + \sum_{j=1}^N W_{i,j}^{(n)}(x)(n_j - n_i) \\ \frac{\partial p_i}{\partial t} &= D_i^{(p)} \Delta p_i + g(n_i, p_i) + \sum_{j=1}^N W_{i,j}^{(p)}(x)(p_j - p_i) \end{aligned} \quad (1)$$

for $i = 1, \dots, N$ where $n_i = n_i(x, t)$ and $p_i = p_i(x, t)$ represent the concentrations of prey and predator population at each time t and position x within the patch $\Omega_i \subset \mathbb{R}^m$, ($1 \leq m \leq 3$), then $\Delta = \sum_{j=1}^m \frac{\partial^2}{\partial x_j^2}$ is the Laplacian operator, $D_i^{(n)}$, $D_i^{(p)}$ are the diffusivity coefficients for prey and predator in every patch Ω_i . The matrices $W_{i,j}^{(n)}(x)$ and $W_{i,j}^{(p)}(x)$ are assumed to be symmetric and their entries represent the migration rates between patches Ω_i and Ω_j for prey and predator, respectively, at position x . We assume that migration occurs only at given positions in the patch which correspond to corridor entrances, and that the corridors have no physical length. By defining as $C_{i,j}$ the entrance of the corridor connecting Ω_i to Ω_j , we have that $C_{i,j} \subset \Omega_i \cap \Omega_j$.

Moreover, we suppose migration rates are constant values in each corridor, i.e. $W_{i,j}^{(n)}(x) = w_{i,j}^{(n)}(x)$ and $W_{i,j}^{(p)}(x) = w_{i,j}^{(p)}(x)$ for every $x \in C_{i,j}$, with $w_{i,j}^{(p)}(x), w_{i,j}^{(n)}(x) > 0$, otherwise $W_{i,j}^{(n)}(x) = W_{i,j}^{(p)}(x) = 0$.

The general form of the reaction terms is

$$f(n, p) = n H(n) - p F(n)$$

(2)

$$g(n, p) = p G(n) - p L(n, p)$$

where the function $H(n)$ is the intrinsic growth rate of prey, $F(n)$ gives the functional response of prey to predator, $G(n)$ is the prey-dependent growth rate of the predator and $L(n, p)$ represents the prey-dependent functional response of predator to the prey. As in Cosner et al. 1996 and Enright 1976 the reaction terms $f(n, p)$ and $g(n, p)$ of LV, RM, May and VT models have different forms for growth according to the following table:

Table II.1 Model functions for the general model

MODEL	$H(n)$	$F(n)$	$G(n)$	$L(n, p)$
LV	r	cn	χcn	δ
RM	$r - \frac{n}{k}$	$\frac{cn}{d + n}$	$\frac{\chi cn}{d + n}$	δ
MAY	$r - \frac{n}{k}$	$\frac{cn}{d + n}$	s	$\frac{qp}{n}$
VT	$r - \frac{n}{k}$	$\frac{cn}{d + n}$	$\frac{\chi cn}{d + n}$	$\delta + \frac{sqp}{n}$

System (1) is completed with suitable initial conditions $n_i(x, 0) = n_{i0}(x)$ and $p_i(x, 0) = p_{i0}(x)$ for $x \in \Omega_i$ and homogeneous Neumann boundary conditions $\frac{\partial n_i}{\partial v_i}(x, t) = \frac{\partial p_i}{\partial v_i}(x, t) = 0$ for $(x, t) \in \partial\Omega_i \times \mathbb{R}$ where v_i is the outward normal vector to the boundary Ω_i $i = 1, \dots, N$. The choice of zero-flux boundary conditions means that the species cannot leave their patches, except via migration. An illustration of the model for $N = 5$ is given in Figure II.2.

The case of a two-patch metapopulation evolving in a two-dimensional space with functions f and g from the RM model and a circular corridor entrance of fixed size was considered in Garvie and Golinski 2010 (see Figure II.3).

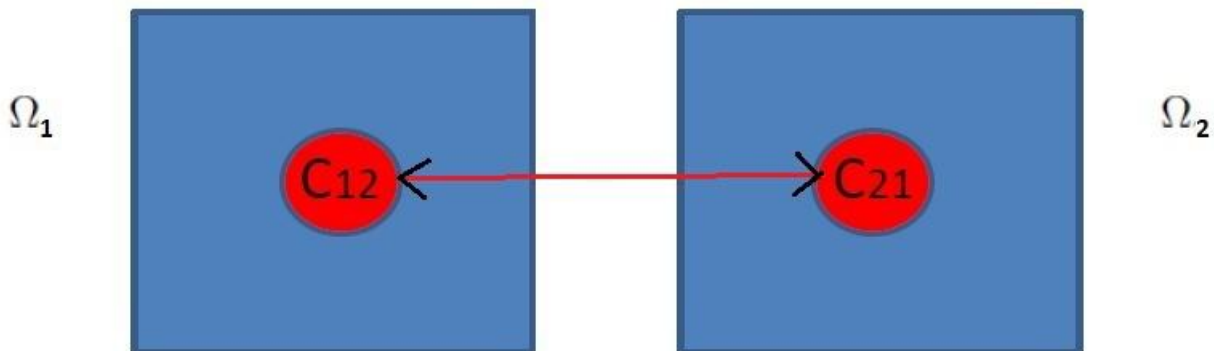


Figure II.3 An illustration of the two-patches two-dimensional metapopulation model with fixed corridor entrance as considered in Garvie and Golinski 2010

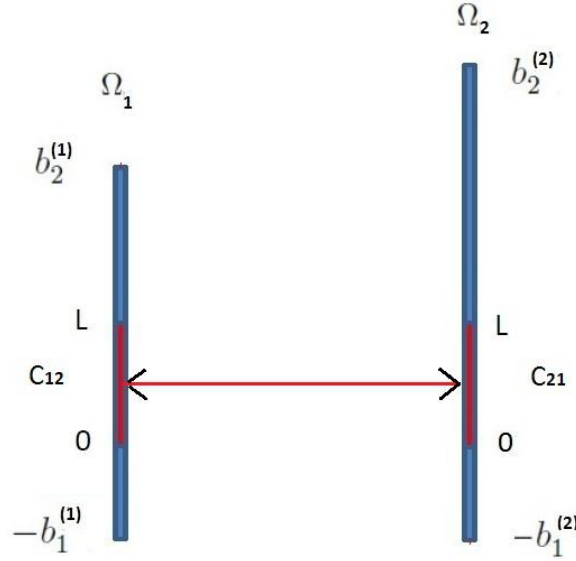


Figure II.4 An illustration of the one-dimensional metapopulation model with two patches Ω_1, Ω_2 and variable corridor entrance size L .

In this paper we restrict our analysis to the two-patch one-dimensional case where the corridor entrances are segments (see Figure II.4). For our purpose we evaluate the change in the dynamics with respect to the length L of the corridor entrance, taken as a parameter. In more detail, let M_1 and M_2 be the length of the two patches we are considering, then we set $C_{1,2} = C_{2,1} = [0, L] \subset \Omega_i = [-b_1^i, b_2^i]$ where b_1^i and b_2^i depend on L according to $b_1^i = (M_i - L)/s$, $b_2^i = ((s - 1)M_i + L)/s$, $i = 1, 2$. Hence, while the domain sizes M_1 and M_2 of both patches are kept constant, the entrance size L of the corridors varies from 0 to $M = \min M_1, M_2$. Of course, in correspondence with $L = 0$ there is no migration and the metapopulation decouples in two separate predator-prey systems. For $L = M$ all positions, at least in one of the two patches, correspond to entrance positions of the corridor.

The model is described as follows

$$\begin{aligned}
 \frac{\partial n_1}{\partial t} &= D_1^{(n)} \Delta n_1 + f(n_1, p_1) + W_{1,2}^{(n)}(x)(n_2 - n_1) \\
 \frac{\partial n_2}{\partial t} &= D_2^{(n)} \Delta n_2 + f(n_2, p_2) + W_{2,1}^{(n)}(x)(n_1 - n_2) \\
 \frac{\partial p_1}{\partial t} &= D_1^{(p)} \Delta p_1 + g(n_1, p_1) + W_{1,2}^{(p)}(x)(p_2 - p_1) \\
 \frac{\partial p_2}{\partial t} &= D_2^{(p)} \Delta p_2 + g(n_2, p_2) + W_{2,1}^{(p)}(x)(p_1 - p_2)
 \end{aligned} \tag{3}$$

where again n_i and p_i are the population concentrations of prey and predators at any time t and position x within the two patches $-b_1^i, b_2^i \subset \mathbb{R}$, $i = 1, 2$.

4.3 The reduced spatially implicit model

In Strohm and Tyson 2011 the authors considered a spatially implicit model that was able to give results similar to the ones provided by the spatially explicit models introduced in Strohm and Tyson 2001.

We follow the same steps in order to deduce systems of ordinary differential equations able to mimic the behaviour of (3).

In order to get the desired model simplification the authors assumed a prey population evolving according to the LV model in a one-dimensional patch $\Omega = [-b_1^i, b_2^i]$ of length M , with homogeneous Dirichlet boundary conditions

$n(-b_1, t) = n(b_2, t) = 0$, in absence of predators. In their frame no migration is accounted for. The equation thus simplifies as follows

$$\frac{\partial n}{\partial t} = D^{(n)} \frac{\partial^2 n}{\partial x^2} + f(n_1, p_1) + rn$$

and it is solved by the method of Fourier series (see e.g. Haberman). The solution is then dominated by the first eigenvalue $\lambda = r - D^{(n)} (\pi/M)^2$, which can be used to discriminate between an exponential growth ($\lambda > 0$) and an exponential decay ($\lambda < 0$) of the prey population. The solution corresponding to the first (principal) eigenvalue can be seen as the exact solution of a ODE

$$\frac{dn}{dt} = (r - D^{(n)} (\pi/M)^2) n$$

with a modified growth rate of the prey which depends on the size of the patch and on the diffusion coefficient $D^{(n)}$ according to the relation

$$r_M = r - D^{(n)} (\pi/M)^2$$

Following the same reasoning, in the absence of prey and migration, the predator population would follow the solution of

$$\frac{\partial p}{\partial t} = D^{(p)} \frac{\partial^2 p}{\partial x^2} - \delta p$$

Hence, we can define the predator death rate as

$$\delta_M = \delta + D^{(p)} (\pi/M)^2$$

and, in the case of the May model, the predator growth rate as

$$s_M = s + D^{(p)} (\pi/M)^2$$

Biologically, the previous assumptions mean that the carrying capacity for each population is dependent of the size M of the patch.

As a final result the original spatially explicit dynamics are converted into implicit ones, by retaining the spatial dependence as patch size dependence for each model parameter.

In the present paper we extend the above approach to the model described in (1) for N patches connected through migration corridors. The growth rates for prey and predator, as well as the death rate of the predator in each patch are changed accordingly. Moreover we attempt to incorporate in the migration rates the dependence on the size L of the corridor.

To this purpose we consider the simplified model

$$\frac{dn_i}{dt} = D_i^{(n)} \frac{\partial^2 n_i}{\partial x^2} - w_{i,j}^{(n)} n_i$$

for $i, j = 1, 2$, with $i \neq j$ and $x \in [0, L]$ and suppose that homogeneous zero Dirichlet boundary conditions are set. The idea is to consider the whole domain as a corridor and to focus on the drop in prey due to the outgoing migration. Hence, we assume that there is no predator in the domain and no contribution comes from the intrinsic growth rate of the prey or to the incoming migration of the population living in the other patch. By assuming that the rate of migration is affected by the first eigenvalue $A_1 e^{-w_{i,j}^{(n)} - D_i^{(n)} (\pi/L)^2}$ of the solution

$$n_i(x, t) = \sum_{m=1}^{\infty} A_m e^{[-w_{i,j}^{(n)} - D_i^{(n)} (\pi/L)^2]t} \sin \frac{m\pi x}{L}$$

we obtain the definition of a new migration coefficient dependent on the size L of the corridor entrance:

$$w_{i,j}^{n,L} = w_{i,j}^{(n)} + D_i^{(n)} (\pi/L)^2 \quad L > 0, \quad w_{i,j}^{n,0} = 0, \quad i, j = 1, 2, \quad i \neq j$$

Similarly, we define

$$w_{i,j}^{p,L} = w_{i,j}^{(p)} + D_i^{(p)} (\pi/L)^2 \quad L > 0, \quad w_{i,j}^{p,0} = 0, \quad i, j = 1, 2, \quad i \neq j$$

Notice that, in the general case, the matrices with entries $w_{i,j}^{(n,L)}$ and $w_{i,j}^{(p,L)}$ are not symmetric.

Finally, we provide the following simplified version of the metapopulation model (3)

$$\begin{aligned}
 \frac{dn_1}{dt} &= n_1 H_{M_1}(n_1) - p_1 F(n_1) + w_{1,2}^{n,L}(n_2 - n_1) \\
 \frac{dn_2}{dt} &= n_2 H_{M_2}(n_2) - p_2 F(n_2) + w_{2,1}^{n,L}(n_1 - n_2) \\
 \frac{dp_1}{dt} &= p_1 G_{M_1}(n_1) - p_1 L_{M_1}(n_1, p_1) + w_{1,2}^{p,L}(p_2 - p_1) \\
 \frac{dp_2}{dt} &= p_2 G_{M_2}(n_2) - p_2 L_{M_2}(n_2, p_2) + w_{2,1}^{p,L}(p_1 - p_2)
 \end{aligned} \tag{4}$$

where, as in Strohm and Tyson 2011, the new functions $H_M(n)$, $G_M(n)$, $L_M(n, p)$ are modified as follows:

Table II.2 Model functions for the metapopulation model

MODEL	$H(n)$	$F(n)$	$G(n)$	$L(n, p)$
LV	r_M	cn	χcn	δ_M
RM	$r_M - \frac{n}{k}$	$\frac{cn}{d+n}$	$\frac{\chi cn}{d+n}$	δ_M
MAY	$r_M - \frac{n}{k}$	$\frac{cn}{d+n}$	s	$\frac{qp}{n}$
VT	$r_M - \frac{n}{k}$	$\frac{cn}{d+n}$	$\frac{\chi cn}{d+n}$	$\delta_M + \frac{sqp}{n}$

4.4 The effect of corridor size variation: comparison between explicit and reduced implicit RM model

We are interested in comparing the influence of reducing the corridor entrance size L on the behaviour of the solution for both the spatially explicit and reduced implicit models. With this aim we vary the size L from the maximum between the patch sizes i.e. $L_{max} = \max\{M_1, M_2\}$ and the minimum value $L_{min} = 0$ which corresponds to separated habitats.

We start from the general system (1) with two patches, where we set $r_i = 1$, $D_i^{(n)} = 1$, $c_i = 1$, $k_i = 1$ ($i = 1, 2$) then we adopt the RM metapopulation model, as in Garvie and Golinski 2010, in order to have

$$\begin{aligned}
 \frac{\partial n_i}{\partial t} &= \Delta n_i + n_i (1 - n_i) - \frac{n_i p_i}{d_i + n_i} + W_{i,j}^{(n)}(x)(n_j - n_i) \\
 \frac{\partial p_i}{\partial t} &= D_i^{(p)} \Delta p_i + \frac{\chi_i n_i p_i}{d_i + n_i} - \delta_i p_i + W_{i,j}^{(p)}(x)(p_j - p_i)
 \end{aligned} \tag{5}$$

for $i, j = 1, 2$, $i \neq j$.

We perform numerical simulations for the solution of this problem in the case of one dimensional patches.

We suppose they have the same dimensions $M_i = 300$ and we set the corridor entrance $[0, L]$ in the center of both domains i.e. $\Omega_i = [(M_i - L)/2, (M_i + L)/2]$, for $i = 1, 2$. We start from the stationary states for predator and prey in Ω_1 and from the stationary state for prey and local extinction of predator in Ω_2 that is

$$n_i(x, 0) = \delta_i d_i / (\chi_i - \delta_i), \quad x \in \Omega_i, \quad i = 1, 2$$

$$p_1(x, 0) = \delta_1 \chi_1 (-\delta_1 + \chi_1 - d_1 \delta_1) / ((\chi_i - \delta_i)^2) \quad x \in \Omega_1$$

$$p_2(x, 0) = 0, \quad x \in \Omega_2$$

The values for the parameters are chosen as follows $d_1 = 1/5$, $\chi_1 = 1$, $\delta_1 = 1/2$, $D_1^{(p)} = 1$, and $d_2 = 2/5$, $\chi_2 = 2$, $\delta_2 = 3/5$, $D_2^{(p)} = 1$.

In order to obtain a numerical approximation for the solution, the Matlab pde solver **pdepe** is exploited: the solver discretizes the equations with respect to the space and then uses the **ode15s** matlab routine for stiff ODEs in order to solve the resulting system. We numerically integrate in the time interval $[0, 250]$ and the solution is plotted in the interval $[200, 250]$, in order to neglect the transient behavior.

In the first simulations we do not consider the prey migration by setting $w^{(n)} = w_{1,2}^{(n)} = w_{2,1}^{(n)} = 0$, then we consider the case $w^{(p)} = w_{1,2}^{(p)} = w_{2,1}^{(p)} = 1$. We find that for $L > 0$ prey and predator spread rapidly throughout the two patches and new dynamics arise; however in the corridor positions prey and predator tend to new equilibria that they reach when the corridor overlaps the whole domain. These approximate equilibrium values are given by $n_1 = 0.7347 \cdot 10^{-8}$, $p_1 = 0.3301$, $n_2 = 0.3306$, $p_2 = 0.4891$. In Figure II.5 we plot the results obtained in correspondence with $L = 10, 150, 200, 300$. In Figure II.6 the same test is done by setting $w^{(p)} = 10^{-6}$.

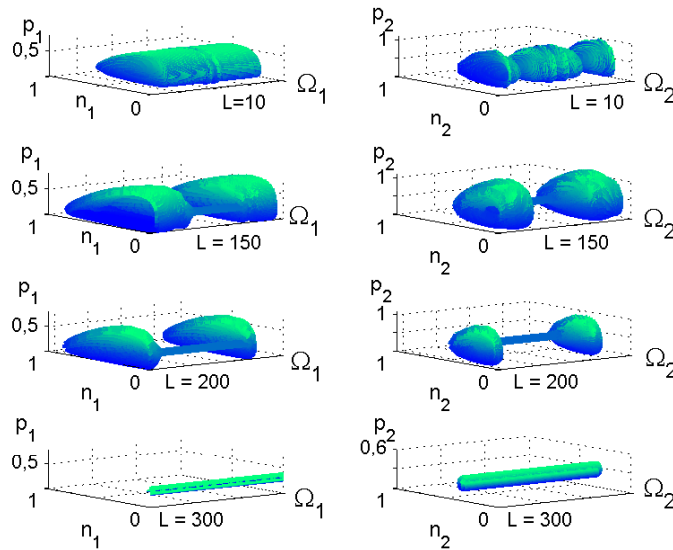


Figure II.5 Spatially explicit RM model: prey-predator dynamics in time interval $[200, 250]$ with $w^{(n)} = 0$ and $w^{(p)} = 1$.

We repeat the same tests with the reduced version of the RM model (5). We slowly vary the size of the corridor and we find that the qualitative behaviour of the implicit model dynamics is approximately the same as the spatially explicit one. For $w^{(n)} = 0$ and $w^{(p)} = 1$, new dynamics arise in correspondence with intermediate values of the corridor size and then new equilibria are reached as it is evident in Figure II.7 on the top (the equilibria values are given by $n_1 = 6.1464 \cdot 10^{-5}$, $p_1 = 0.3249$, $n_2 = 0.3500$, $p_2 = 0.4873$). The results shown in Figure II.7, on the bottom, are obtained by setting $w^{(p)} = 10^{-6}$ and confirm the behavior of the predator-prey population predicted by the spatially explicit model: as soon as the size of the corridor is strictly positive we observe the prey-predator dynamics spreads in both patches till the prey-predator populations reach limit cycles when the corridor takes the same size of the domain.

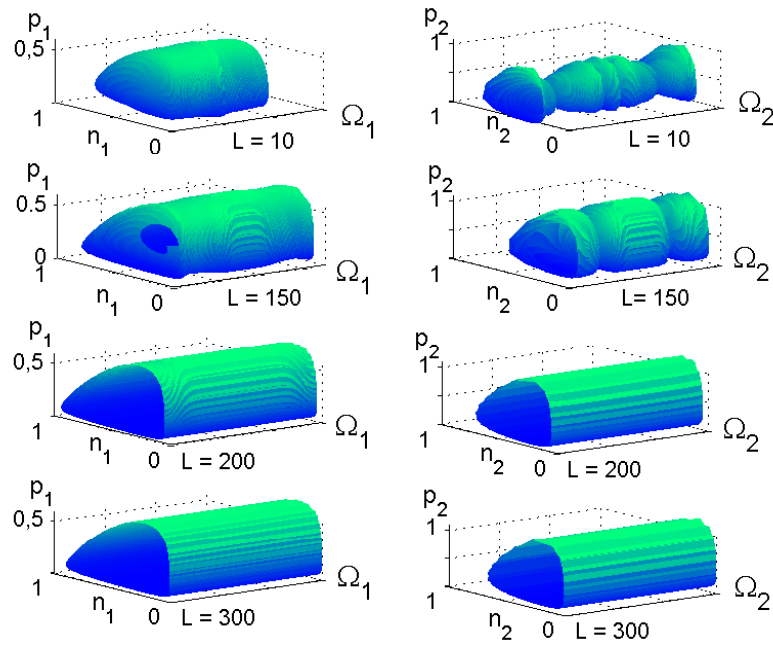


Figure II.6 Spatially explicit RM model: prey-predator dynamics in time interval $[200, 250]$ with $w^{(n)} = 0$ and $w^{(p)} = 1e - 6$.

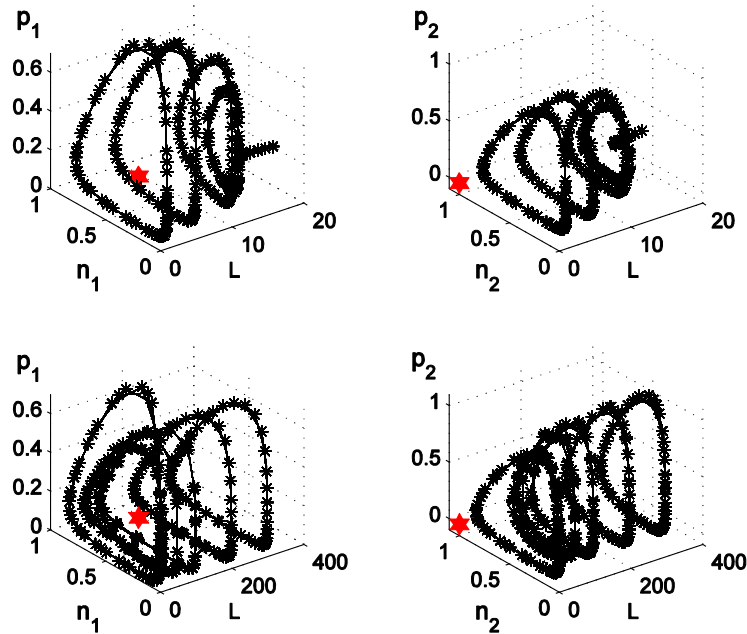


Figure II.7 Reduced implicit RM model: prey-predator dynamics in time interval $[200, 250]$ with $w^{(n)} = 0$, $w^{(p)} = 1$ on the top and $w^{(p)} = 1e - 6$ on the bottom.

4.5 The effect of corridor size variation: comparison among different reduced implicit models

By means of the reduced implicit models we numerically investigate the change in the cyclic population dynamics as a function of the variation of both the domain size M_i and the corridor length L . The general model (1) has

been considered with the four different expressions of the reaction terms. The parameters of the model corresponding to the two patches at hand are given in Tables II.3 and II.4

Table II.3 *Parameters values related to patch Ω_1*

Ω_1								
Parameters	r	c	χ	δ	d	s	q	k
LV	0.75	122	0.00197	0.85				
May	1.75	505			0.3	0.85	212	8
RM	2.1	800	0.004	2.4	1.5			11
VT	1.75	800	0.004	2.4		0.8	212	8

Table II.4 *Parameters values related to patch Ω_2*

Ω_2								
Parameters	r	c	χ	δ	d	s	q	k
LV	1	120	0.002	1				
May	2	400			0.1	1	100	10
RM	3	750	0.004	3	1			10.5
VT	2	750	0.004	2.1		1	200	10

We start with initial conditions $n_1(0) = 7$, $n_2(0) = 3$, $p_i(0) = 0.01$, for $i = 1, 2$. In the first test two domains of the same size $M_i = 50$ are considered with diffusive coefficients given by $D_i^{(n)} = 1.5$ and $D_i^{(p)} = 2$, $i = 1, 2$. In order to compare the results provided by the four different approaches, we measure the average population density and population cycle amplitude in both patches. As in Strohm and Tyson 2011, the average density is obtained by averaging the maximum and the minimum population densities, then the cycle amplitude is evaluated by taking the difference between the maximum and the minimum densities. The obtained results are shown in Figures II.8 and II.9 for migration rates $w^{(n)} = w^{(p)} = 1$. We observe that prey and predator populations, for every $L > 0$ spread throughout the two domains and synchronize their respective orbits. If we repeat the same test with different domain size we obtain similar results. By setting $w^{(n)} = w^{(p)} = 1e - 6$, we obtain the results shown in Figures II.10 and II.11: we notice that now the corridor size has a major effect on the dynamics. Indeed, for small values of corridor sizes we have huge values of migration rates and prey and predators immediately show dynamics similar to the one obtained in the first test. However, for increasing values of L the migration rates decrease fast converging to the constant value $1e - 6$. In correspondence with these values of migration rates new dynamics may appear accordingly with the maximum size of the corridor and, in turns, with the maximum size of the smallest domain. Indeed, if we repeat the same test for two domains of different size, $M_1 = 50$ and $M_2 = 5$, we have the results provided in Figures II.12 and II.13.

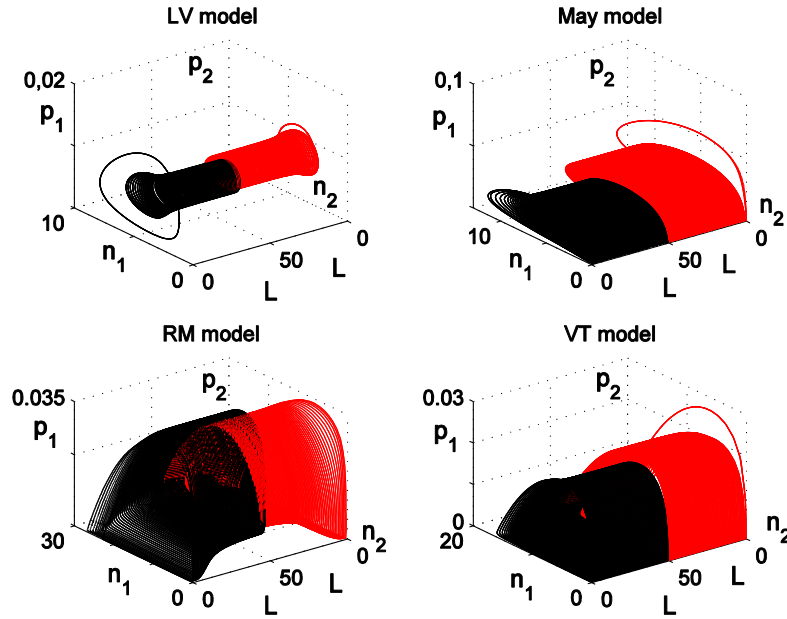


Figure II.8 Spatially explicit model: prey-predator dynamics w.r.t. corridor size $0 \leq L \leq M_1 = M_2 = 50$ with $w^{(n)} = 0$ and $w^{(p)} = 1$.

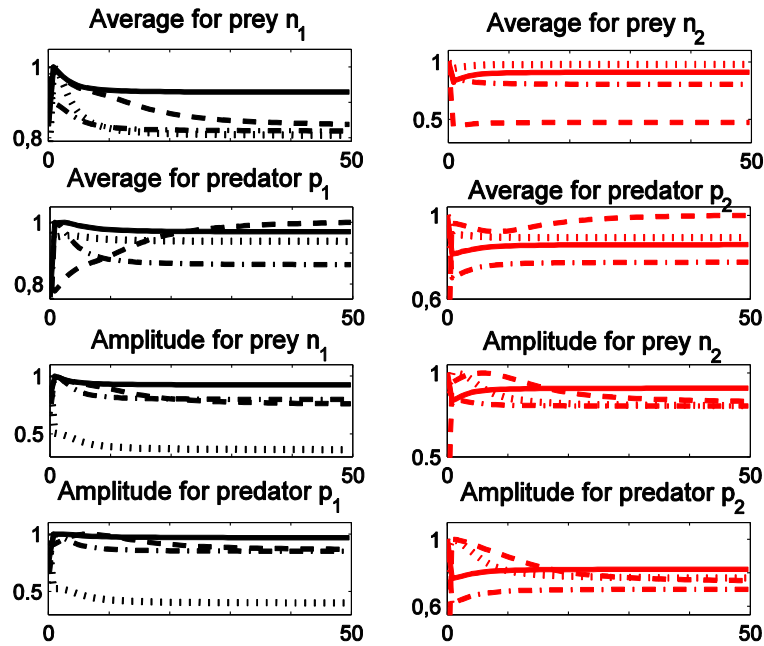


Figure II.9 Spatially explicit model: prey-predator average and amplitude w.r.t. corridor size $0 \leq L \leq M_1 = M_2 = 50$ with $w^{(n)} = 0$ and $w^{(p)} = 1$. LV model: dotted line, May model: dash-dotted line, RM model: dashed line, VT model: solid line

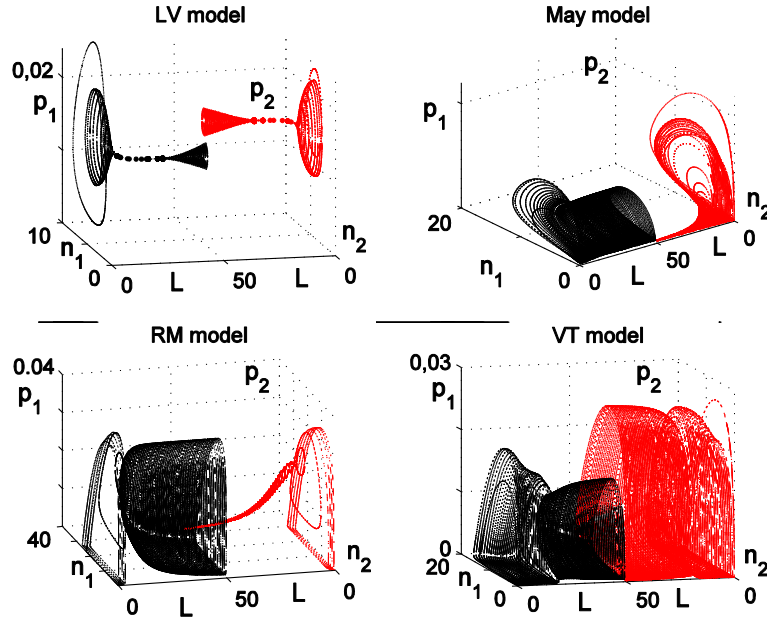


Figure II.10 Spatially explicit model: prey-predator dynamics w.r.t. corridor size $0 \leq L \leq M_1 = M_2 = 50$ with $w^{(n)} = 0$ and $w^{(p)} = 1e - 6$.

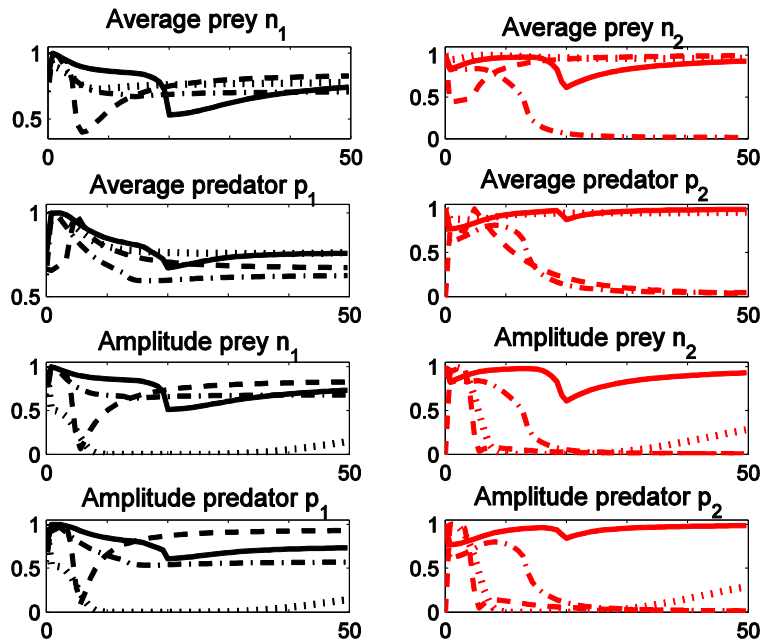


Figure II.11 Spatially explicit model: prey-predator average and amplitude w.r.t. corridor $0 \leq L \leq M_1 = M_2 = 50$ with $w^{(n)} = 0$ and $w^{(p)} = 1e - 6$. LV model: dotted line, May model: dash-dotted line, RM model: dashed line, VT model: solid line.

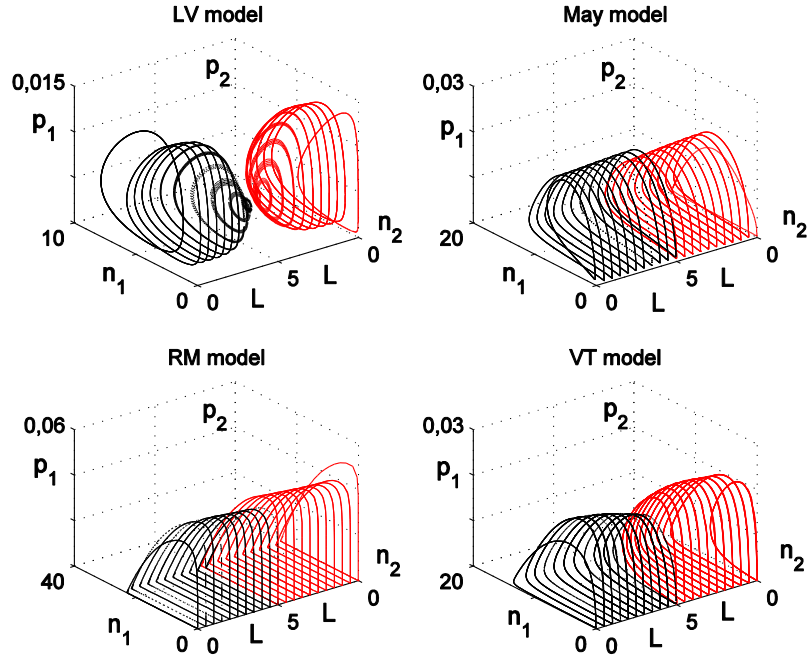


Figure II.12 Spatially explicit model: prey-predator dynamics w.r.t. corridor size $0 \leq L \leq M_2 = 5$ with $w^{(n)} = 0$ and $w^{(p)} = 1e - 6$.

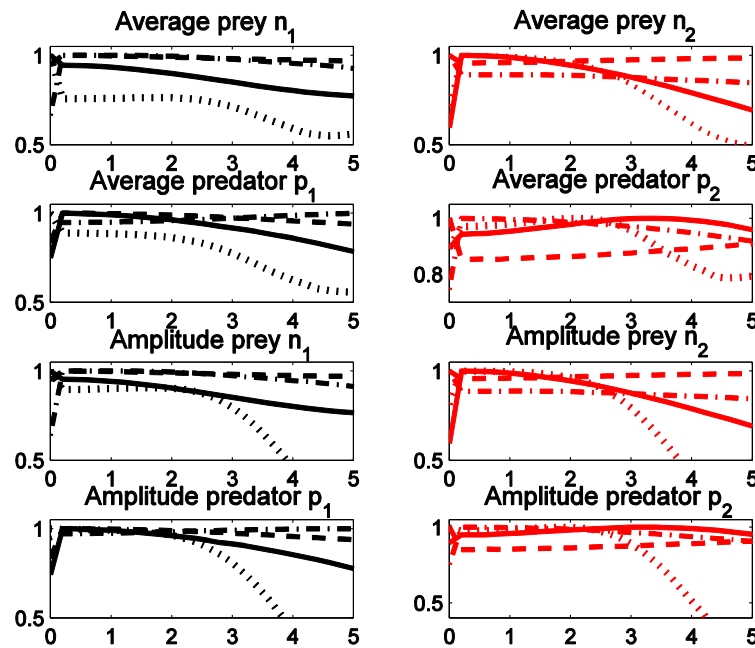


Figure II.13 Spatially explicit model: prey-predator average and amplitude w.r.t. corridor size $0 \leq L \leq M_2 = 5$ with $w^{(n)} = 0$ and $w^{(p)} = 1e - 6$. LV model: dotted line, May model: dash-dotted line, RM model: dashed line, VT model: solid line

4.6 Part II. Conclusions and recommendations

The analysis of spatial processes in ecological systems allows us to set up theoretical models which may provide results closer to the real investigated phenomena.

Indeed, merely focusing on individual patches would not give a sufficient idea of resilience or threat at the metapopulation level. This approach provides a way to go beyond this limitation especially when the extension of singular patches is not suited for hosting a viable and stable population of predators, as it is the case of the BIO_SOS Alta Murgia study site.

The domain and the corridor size are fundamental in order to study the effect of habitat fragmentation on population dynamics; indeed as well as in too small patches the population cannot survive, and similarly in too small corridors the migration is reduced and new dynamics arise. In this paper, a first numerical investigation about the effect of the reduction of the corridor size in metapopulation cyclic dynamic has been provided. By focusing on the one dimensional two-patch case, we performed some numerical test on the spatially explicit model introduced in Garvie and Golinski 2010; thus, by following the approach proposed in Strohm and Tyson 2011, we proposed a reduced spatially implicit model where the size of both the domain and the corridor are taken into account by means of nonlinear relationships that interlace growth and migration rates with diffusive coefficients which define the spatially explicit model. Our results confirm that the proposed implicit model reproduces well the qualitative behavior of the related spatially explicit one. Finally, the effect of corridor size variation in two-patches with different domain dimensions is also investigated: we compared four classical models found in literature and, as a result, we found that variation of the corridor size may affect the dynamics for given parameters values. All the results are obtained by means of standard numerical tools implemented in Matlab routines. Future work will deal with ad hoc numerical techniques which are able to face the problem with two-dimensional patches, whose numerical simulation is very expensive, with the aim of verifying the results we have just obtained in one-dimension two-patch systems.

5. Appendix

5.1 Appendix 1: Acronym list

DESIRE	Desertification mitigation and remediation of land – a global approach for local solutions
DTM	Digital Terrain Model
EO	Earth Observation
EUROSEM	European Soil Erosion Model
Grass	Geographic Resources Analysis Support System
HR	High Resolution
LANDPLANER	Landscape, Plants, Landslide and Erosion Model
LC	Land Cover
LC/LU	Land cover / land use
LCC	Land Cover Change
MWISED	Modelling Within Storm Erosion Dynamics
NRCS Runoff	Curve Number method
RECONDES	Conditions for Restoration and Mitigation of Desertified Areas Using Vegetation
SDMs	Species distribution models
SPEC	Species of European Conservation Concern
VHR	Very High spatial Resolution

6. References

- Baggio J.A., Salau K., Janssen M.A., Schoon M.L., Bodin O., Landscape connectivity and predator-prey population dynamics, *Landscape Ecology*, 26, pp. 33-45, 2011.
- Conroy M.J., Cohen Y., James F.C., Matsinos Y.G., Maurer B.A., Parameter-estimation, reliability, and model improvement for spatially explicit models of animal populations, *Ecological applications* 5, pp. 17–19, 1995.
- Cosner C., Variability, vagueness and comparison methods for ecological models, *Bulletin of Mathematical Biology*, 58(2), 1996, pp. 207–246.
- De Baets, S., Torri, D., Poesen, J., Salvador, M.P., Meersmans, J., 2008. Modelling increased soil cohesion due to roots with EUROSEM. *Earth Surface Processes and Landforms* 33(13): 1948-1963, published online in Wiley InterScience, (www.interscience.wiley.com) DOI: 10.1002/esp.1647.
- Dunning J.B., Stewart D.J., Danielson B.J., Noon B.R., Root T.L., Lamberson R.H., Stevens E.E., Spatially explicit population models - current forms and future uses, *Ecological Applications* 5, pp. 3–11, 1995.
- Enright J., Climate and population regulation. The biogeographer's dilemma, *Oecologia*, 24(4), pp. 295–310, 1976.
- Fahrig L., Effects of habitat fragmentation on biodiversity, *Annu. Rev. Ecol. Evol. Syst.*, 34, pp. 487–515, 2003.
- Garvie M.R., Golinski M., Metapopulation dynamics for spatially extended predator-prey interactions, *Ecological Complexity*, 7, pp. 55–59, 2010.
- Haberman R, *Applied partial differential equations*, Prentice-Hall, Upper Saddle River.
- Hawkins, R.H., Ward, T.J., Woodward, D.E., Van Mullem, J.A., 2009. *Curve Number Hydrology -State of practice*. ASCE publication, ISBN 978-0-7844-1004-2, 106 pages.
- Huffaker C.B., Experimental studies on predation: dispersion factors and predator-prey oscillation, *Hilgardia*, 27, pp. 343–383, 1958.
- Jansen V.A.A., The dynamics of two diffusively coupled predator-prey populations, *Theoretical Population Biology*, 59, pp. 119–131, 2001.
- Levins, R. (1969), Some demographic and genetic consequences of environmental heterogeneity for biological control, *Bulletin of the Entomological Society of America*, 15, pp. 237–240, 1969.
- May R., *Stability and complexity in model ecosystems*, Princeton University Press, Princeton, 1974.
- Menéndez-Duarte R., Marquínez J., Fernández-Menéndez, S., Santos, R., 2007. Incised channels and gully erosion in Northern Iberian Peninsula: Controls and geomorphic setting . *Catena*, 71: 267-278.
- Minor E.S., Urban D.L., Graph theory as a proxy for spatially explicit population models in conservation planning, *Ecological Applications*, 17(6), pp. 1771–1782, 2007.
- Montgomery, D.R., and Dietrich, W.E., 1994. Landscape dissection and drainage area-slope thresholds – Chapter 11. In Kirkby, M.J. (ed.) *Process models and theoretical geomorphology*, John Wiley & Sons Ltd., 221-246.
- Morgan, R.P.C., Quinton, J.N., Smith, R.E., Govers, G., Poesen, J.W.A., Auerswald, K., Chisci, G., Torri, D. and Styczen, M.E., 1999. Reply to discussion on The European soil erosion model (EUROSEM): a process-based approach for predicting soil loss from fields and small catchments. *Earth Surface Processes and Landforms*, 24, 567-568.
- NRCS, 2004. Chapter 9: Hydrologic Soil-Cover Complexes. Part 630 Hydrology, *National Engineering Handbook*.
- Okubo A., Levin S.A., *Diffusion and ecological problems: modern perspectives*, Springer, New York, 2001.
- Patton, P.C., and Schumm S.A., 1975 . Gully Erosion, Northwestern Colorado: a threshold phenomenon. *Geology*, 3, 88-90.
- Poesen, J.W.A., Torri ,D., and Vanwalleghe, T., 2011. Gully erosion: procedures to adopt when modelling soil erosion in landscapes affected by gullyng. Chpt. 19, in Morgan, R.P.C. & M.A. Nearing (eds) *Handbook of Erosion Modelling*. ISBN: 978-1-4051-9010-7, Hardcover, 416 pages, 2011, Wiley-Blackwell, 360-386.

Rosenzweig M., MacArthur R., Graphical representation and stability conditions of predator-prey interactions, *The American Naturalist*, 97, pp.209–223, 1963.

T. Smets, L. Borselli, J. Poesen, D. Torri. 2011. Evaluation of the EUROSEM model for predicting the effects of erosion-control blankets on runoff and interrill soil erosion by water. *Geotextiles and Geomembranes*, 29; 285-297.

South A., Dispersal in spatially explicit populations models, *Conservation Biology*, 13, pp. 1039–1046, 1999.

Strohm S., Tyson R., The effect of habitat fragmentation on cyclic population dynamics: a numerical study, *Bulletin of Mathematical Biology*, 71, pp. 1323–1348.

Strohm S., Tyson R., The effect of habitat fragmentation on cyclic population dynamics: a reduction to ordinary differential equations, *Theoretical Ecology*, DOI 10.1007/s12080-011-0141-1 (published online: 20 October 2011).

Torri D. and Poesen J., (to be submitted) A review of topographic threshold conditions for gully head development in different environments.

Turchin P., Batzli G., Availability of food and the population dynamics of arvicoline rodents, *Ecology*, 82, pp. 1521–1534, 2001.

Turner M.G., Arthaud G.J., Engstrom R.T., Hejl S.J., Liu J.G., Loeb S., McKelvey K., Usefulness of spatially explicit population models in land management, *Ecological Applications*, 5, pp. 12–16, 1995.

Urban D., Keitt T., Landscape connectivity: a graph-theoretic perspective, *Ecology*, 82, pp. 1205–1218, 2001.

Vandekerckhove, L., Poesen J., Oostwoud-Wijdene, D., Nachtergaele, J., Kosmas, C., Roxo, M.J., and de Figueiredo, T., 2000. Thresholds for gully initiation and sedimentation in Mediterranean Europe, *Earth Surface Processes and Landforms*, 25, 1201-1220.

Wu, Y. & Cheng, H. (2005) Monitoring of gully erosion on the Loess Plateau of China using a global positioning system. *Catena* 63: 154–66.